Growth and structure of thin Au films on Ag(111)

B. Eisenhut, J. Stober, G. Rangelov, and Th. Fauster
Sektion Physik, Universität München, Schellingstraße 4, 80799 München, Germany
(Received 29 November 1993)

The growth and the structure of thin Au films on Ag(111) were studied by measuring the angular distribution of core-level photoelectrons emitted at high kinetic energy using a two-dimensional display-type electron spectrometer. Additional information was obtained by angle-integrated photoelectron spectroscopy and by thermal desorption spectrometry of NO. We find, even at room temperature, intermixing induced by surface diffusion. This conclusion is corroborated by the study of Au films deposited on (1–3)-monolayer-high Ag films grown on Pd(111).

I. INTRODUCTION

The growth of ultrathin metal films has many important technological applications. Usually flat, smooth, and closed films are desirable which are, however, often not achieved. From thermodynamic considerations the requirement for this layer-by-layer growth is that the surface free energy of the film is lower than the surface free energy of the substrate.[1] Additional terms to be included are the interfacial energy and the strain energy of the stressed epitaxial film. Even if the thermodynamic preconditions for layer-by-layer growth are met, one often finds film growth different from the expected behavior.[2,3] The explanation is that film growth usually occurs far away from thermodynamic equilibrium. Kinetic terms keep the deposited atoms from reaching their thermodynamically optimum position. Further complications arise from the altered bonding configuration at the surface which can lead to an incorporation of deposited atoms into the surface,[2,4,5] even for immiscible systems.[6]

We have studied the epitaxial growth of thin Au films on the close-packed (111) surface of Ag. These noble metals should constitute a particularly simple prototype system for the various growth modes. Gold and silver are chemically very similar and crystallize both in the face-centered-cubic (fcc) lattice structure with almost identical lattice constants. These properties should minimize the interfacial energy and the strain energy of the film. An intermixing at the interface seems unlikely for close-packed fcc (111) surfaces.

The growth of Au on Ag(111), however, has been up to now discussed controversially in the literature. A low-energy electron diffraction (LEED) investigation[7] asserted that upon the deposition of 2.5 monolayers Au on Ag(111) the growth of the Au film can proceed under apparently the same growth conditions in two different ways: layer-by-layer growth or diffusion of Ag during Au deposition. In another study based on high-energy ion scattering and Auger electron spectroscopy (AES) Culbertson *et al.*[8] interpret their data by a growth of the Au films on Ag(111) in a layer-by-layer mode with a well-defined atomically abrupt interface. Meinel, Klaua, and Bethge[9] infer from their AES results an island growth with a Poisson distribution of the terrace heights (simultaneous multilayer growth).[2] This growth mode and also growth in a layer-by-layer fashion are, however, excluded by an investigation using low-energy alkali ion scattering spectroscopy and AES by Mahavadi.[10] He suggests an alloying at the interface of Au on Ag(111) in agreement with earlier work of Gruzza, Guglielmacci, and Gillet.[11] A similar conclusion is reached in the photoemission work of Lipphardt *et al.*[12]

The deposition of Au on thin Ag films on Pd(111) raises the possibility of obtaining information about the range of influence of the substrate on the growth behavior. This knowledge is important for multilayer structures. Results for the growth and the structure of thin Ag films on Pd(111) have been reported previously.[13] At room temperature Ag grows epitaxially on Pd(111) in a layer-by-layer mode, which has been confirmed by a two-photon photoemission investigation.[14] The first Ag layer grows pseudomorphically, followed by a stacking fault between the first and the second layer related to the compensation of the lattice mismatch. Palladium has a $\sim 5\%$ smaller lattice constant than Ag and Au. Thick Ag films show a fcc crystal structure with the Ag lattice constant, are almost as well ordered as the Pd(111) substrate, and grow in (111) twin orientation with respect to the substrate. Growing Au layers on the compressed pseudomorphic first Ag layer might give insight into the importance of the lattice mismatch for the growth behavior.

The main experimental technique used was photoelectron forward scattering which is particularly suitable to yield direct information on the growth and structure of thin films on single-crystal metal surfaces.[15–18] For the study of complex growth behavior it is important to sample the complete angular distribution of the photoelectrons at high kinetic energies[19,20] which can be most easily done using a two-dimensional display-type electron spectrometer.[21] These experiments were complemented by angle-integrated photoemission, thermal desorption spectrometry (TDS), AES, and LEED.

II. EXPERIMENT

Sample preparation, TDS, AES, and LEED measurements were performed in a separate ultrahigh vacuum chamber which is connected to the chamber of

the display-type analyzer[21] by a transfer system. The Pd(111) and Ag(111) crystals were cleaned following standard procedures.[13,22] The surface cleanliness and crystallographic order were verified with AES, TDS, and LEED. Gold and silver were evaporated from tungsten baskets at a rate of 0.01 monolayers (ML) per second onto the substrates at room temperature ($\leq 50\,^{\circ}C$) and at a pressure of $< 2 \times 10^{-10}$ mbar. Coverages are given in monolayer equivalents and were determined with an uncertainty of 10 % by means of a calibrated quartz microbalance.

For the forward-scattering experiments synchrotron radiation with an energy of typically 900 eV from the HE-TGM-1 beam line at the BESSY (Berliner-Elektronenspeicherring-Gesellschaft für Synchrotronstrahlung) storage ring was employed. The angular distribution patterns (ADP's) of the photoelectrons were recorded by a two-dimensional display-type electron spectrometer[21] which allows us to measure simultaneously the complete angular distribution in an acceptance cone of 88°. The data processing and the normalization with respect to the spatial analyzer efficiency have been described previously.[13,19] The ADP's are presented in the form of gray-scale pictures. In order to show the structures as clearly as possible, the lowest (highest) intensity of each ADP is shown in the picture as black (white).

III. ANGLE-INTEGRATED SPECTROSCOPIES

A. Angle-integrated photoelectron spectroscopy

To study the growth mode of thin films we present first the results of the angle-integrated x-ray photoelectron spectroscopy (XPS) measurements. In these experiments we determine the relative intensities and inelastic contributions by a line-fitting procedure using the spectra from the clean Ag(111) and Pd(111) surfaces and from an 8 ML thick Au film on Ag(111) as reference (compare to Ref. 19). The kinetic energy of the electrons from the Ag 3*d*, Pd 3*d*, and Au 4*d* core levels was 519, 551, and 546 eV, respectively. The film signal normalized to the sum of film and substrate signal is shown in the center of Fig. 1 for Ag on Pd(111) and Au on Ag(111). It is evident that at low coverages the values of Au/(Au+Ag) are always smaller than those of Ag/(Ag+Pd). If both systems have the same growth mode, the differences between the data would imply a mean free path ~ 1.4 times larger for the Au on Ag(111) system compared to the Ag on Pd(111) system. This factor is too large to be explained by the slight differences in the kinetic energy or by dependence on the adsorbate material.[23] Therefore, the growth mode for Au on Ag(111) cannot be layer by layer, the growth mode established for Ag on Pd(111).[13]

In order to clarify the growth mode, we have performed model calculations using the formalism proposed by Ossicini, Memeo, and Ciccacci.[24] The Ag/(Ag+Pd) data show good agreement with the curve calculated for layer-by-layer growth (dashed line in Fig. 1) with a mean free path of 9.1 Å. This value is used for the calculations of other growth modes. The solid line in Fig. 1 corresponds to a Poisson distribution of the terrace heights (diffusion-limited simultaneous multilayer growth)[2] and does not agree with the experimental data for Au on Ag(111). Therefore, either Au must grow in islands which are considerably higher than for simultaneous multilayer growth or there must be an intermixing between Au and Ag.

The latter hypothesis is confirmed by inspection of the inelastic intensity due to electrons from deeper layers which have lost energy on their way to the surface (top part of Fig. 1). The loss intensity is normalized to the integral yield of the elastic peak. For Ag on Pd the loss intensities increase with coverage. The linear increase for the Pd signal (open diamonds) indicates that the electrons emitted from Pd atoms have to traverse a Ag layer of increasing thickness. The Ag signal (filled diamonds)

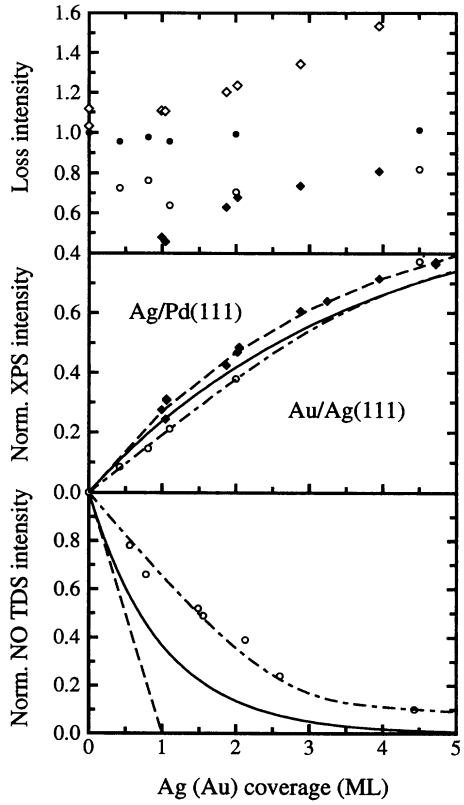

FIG. 1. Center: Variation of the XPS intensity ratio Au/(Au+Ag) (open circles) and Ag/(Ag+Pd) (filled diamonds) as a function of Au coverage. The data were normalized relative to clean surfaces or thick films. The kinetic energy of the Au 4*d*, Ag 3*d*, and Pd 3*d* electrons was 546, 519, and 551 eV, respectively. Top: Inelastic energy loss intensity for Au on Ag(111) (open and filled circles for the Au 4*d* and the Ag 3*d* core level, respectively) and for Ag on Pd(111) (open and filled diamonds for the Pd 3*d* and the Ag 3*d* core level, respectively). Bottom: Thermal desorption of NO from Ag(111) (open circles) as a function of Au coverage. The data were normalized with respect to the yield of clean surfaces. All measurements were taken after a saturation exposure to NO at room temperature. Additionally, model curves are shown for simultaneous multilayer growth (solid lines), alloy formation (dash-dotted lines), and layer-by-layer growth (dashed lines).

approaches the bulk value at a thickness corresponding to a few times the mean free path. The situation is completely different for Au on Ag(111) where the loss signal from both the adsorbate and the substrate stay almost constant. The high value of the Au loss intensity (open circles) at low coverages indicates that Au atoms must already be in deeper layers. The low value of the Ag loss intensity (filled circles) at high coverages indicates that Ag atoms must still be in the top layers. The latter behavior is compatible only with a partial intermixing between Ag and Au leading to a partial buildup of Ag on top of Au. We note that the conclusion about the growth mode is supported by our AES results[25] which are in good agreement with those of other authors.[8–10]

B. Thermal desorption spectrometry

Thermal desorption spectrometry of NO was used to monitor the concentration of the Au atoms in the uppermost layer. Since NO does not adsorb on Au at room temperature,[26] in contrast to Ag(111),[27] the total NO desorption yield is a measure of the uncovered Ag atoms at the surface. The desorbing NO was detected by a mass spectrometer and registered by a computer. The total yield was obtained by numerical integration after a suitable background subtraction. In Fig. 1 (bottom part) the normalized total TDS yield of NO from Au/Ag(111) is shown as a function of the Au coverage. The data were normalized to the yield of the clean surfaces. The data deviate from the straight dashed line which is expected for layer-by-layer growth. This behavior is found for Ag on Pd(111) where no desorbing CO [at room temperature NO adsorbs on Ag and Pd, whereas CO adsorbs on Pd (Ref. 28) but not on Ag (Ref. 29)] could be detected at a Ag coverage of 1.2 ML. The solid line shows the decrease of the uncovered fraction of the surface assuming that simultaneous multilayer growth occurs. For NO/Au/Ag(111) much more uncovered Ag atoms exist than indicated by this model. This confirms the conclusion about alloy formation of the preceding section.

C. Alloy model

The Au/(Au+Ag) data set was fitted by a model (shown by the dash-dotted lines in Fig. 1) in which the alloy formation is considered as a diffusion process of the atoms between a semi-infinite Ag crystal and a finite Au reservoir.[30] Assuming that the diffusion constant is independent of the concentration, the solution of the diffusion equation gives the concentration of the Au atoms in each layer of the film at a particular Au coverage. This concentration profile was inserted into the formalism of Ossicini, Memeo, and Ciccacci[24] and fitted to the XPS data. The mean free path of electrons at kinetic energies around 550 eV has been determined by a fit of a layer-by-layer growth model to the data for Ag on Pd(111) (dashed line in Fig. 1, center). The remaining parameter is the diffusion constant which was obtained as $0.9 \pm 0.4 \times 10^{-19}$ cm^2/s in agreement with the literature.[11] This diffusion model (dot-dashed line) describes the XPS data of Fig. 1 very well. The concentration of the Ag atoms at the surface determined on the basis of the alloy formation (dot-dashed line in Fig. 1, bottom) agrees quantitatively with the experimental TDS data.

This diffusion model describes the experimental data fairly well, but it should be regarded with caution. It implies a continuous change of the concentration with time. For the time entering the model we used the typical time ($\sim$ 30 min) between sample preparation and the actual measurement. Even though we have not undertaken specific studies, we have, however, no indication for time-dependent changes of the samples at room temperature in agreement with Ref. 31. Therefore, it might be just coincidental that a diffusion model with a suitable choice of the diffusion constant yields a satisfactory description of the experimental data.

IV. ANGLE-RESOLVED PHOTOELECTRON SPECTROSCOPY

A. Forward scattering

Core-level photoelectrons with a kinetic energy of some hundred eV exhibit enhanced intensity along the internuclear axes connecting the emitting atom with its neighbor atoms due to forward scattering.[15–18] The angular distribution of these photoelectrons yields, therefore, structural information which can be obtained by a straightforward geometrical interpretation. Figure 2 (left part) shows a side view normal to the (111) surface of a fcc crystal [$(1\bar{1}0)$ plane]. It illustrates the crystallographic directions where the forward scattering of the photoelectrons at neighbor atoms causes enhanced intensity. In

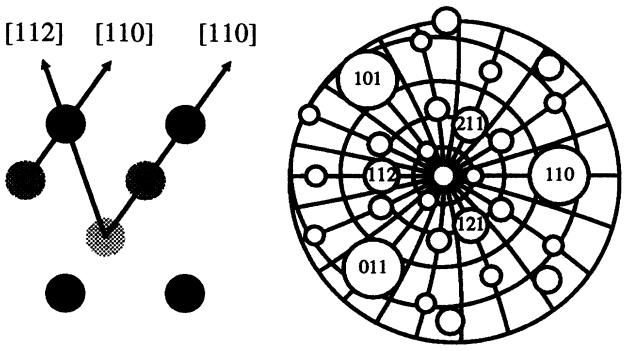

FIG. 2. (Left) Side view normal to the (111) surface of a fcc crystal [$(1\bar{1}0)$ plane] to illustrate the dense packed, low-index crystallographic directions which correspond to the expected intensity maxima in the forward-scattering experiment. (Right) The expected angular distribution of photoelectrons for a fcc (111) surface due to the forward scattering of the electrons by the neighbor atoms along the crystal directions given by the numbers. The center of the angular grid corresponds to normal emission [(111) direction]. The separation between the lines of the grid is 10° and 15° for the polar and azimuthal directions, respectively.

the right part of Fig. 2 the forward-scattering directions for a fcc (111) surface are plotted in the angular grid of the display-type analyzer. The area of the circles is proportional to the square of the distance between the emitter and the scatterer and corresponds, therefore, roughly to the expected intensity. The numbers give the crystal directions between emitter and scatterer.

The concept of photoelectron forward scattering is illustrated in Fig. 3 by the angular distribution patterns for the clean Pd(111) surface and an 8 ML thick Au film grown on Ag(111). Enhanced intensity along the ⟨110⟩ and ⟨112⟩ directions (compare to Fig. 2) can be clearly identified. The ADP's are a direct image of the directions of the high-density atom chains in real space. In addition to the intensity maxima in the forward-scattering directions there exist bands connecting the intensity maxima in the ⟨110⟩ directions. These bands have also been observed in the ADP's of other fcc metals and can be interpreted in terms of Kikuchi bands.[20]

The comparison of the forward-scattering patterns from different core levels (Pd 3*d*, Au 4*d*, and Au 4*f*) at kinetic energies around 550 eV reveals no significant differences. One might expect an influence of the angular momentum of the core level,[20,32] especially with excitation by polarized synchrotron radiation. The absence of large differences proves that the ADP's are dominated by forward scattering and represent primarily the geometric structure of the surface. The two ADP's from the Au 4*f* core level shown in the bottom of Fig. 3 measured at kinetic energies of 559 and 803 eV exhibit clear differences. The forward-scattering directions appear in both patterns, but the picture at higher kinetic energies is much clearer and sharper. This illustrates that the forward scattering occurs in a narrower cone with increasing energy.[15,32] The Kikuchi bands also become more pronounced at higher kinetic energy, which reflects the larger mean free path of the electrons. It would be interesting to see whether these statements can be corroborated by calculations.

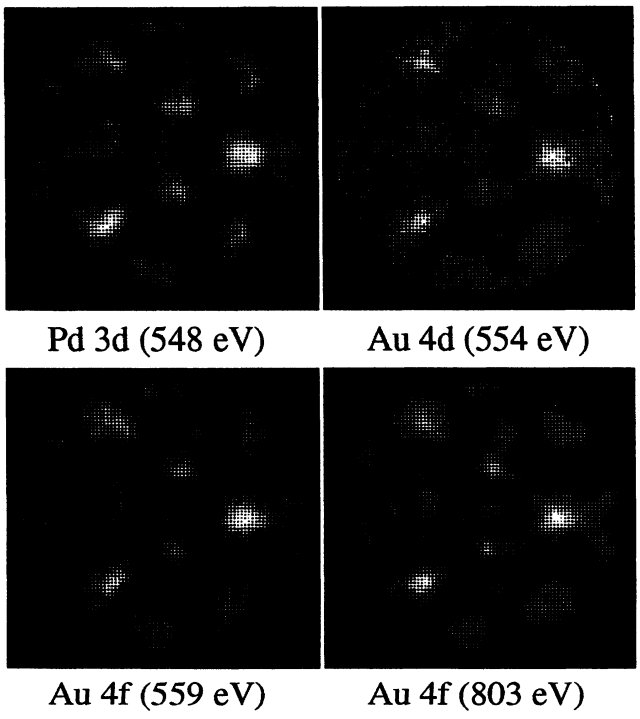

FIG. 3. Comparison of the experimental angular distributions of photoelectrons for different core levels Pd 3*d*, Au 4*d*, and Au 4*f* at a kinetic energy around 550 eV. For a kinetic energy of 803 eV the forward scattering becomes more pronounced. The data were obtained for the clean Pd(111) surface and for an 8 ML thick Au film on Pd(111).

B. Film growth

In Fig. 4 we present the ADP's after deposition of various amounts ($\sim 1, 2$, and 4 ML) of Ag on Pd(111) and Au on Ag(111). All data were taken at a photon energy of ≈ 900 eV which gives kinetic energies of 519 and 810 eV for the electrons of the Ag 3*d* and Au 4*f* core levels, respectively. All patterns show emission from the film material, except the one in the lower right corner which is from the clean Ag(111) surface.

The data for Ag on Pd(111) (top row in Fig. 4) have been presented in part before.[13] They are reproduced here to illustrate the differences from the Au on Ag(111) system and for comparison to the data of Sec. IV C. For 1.0 ML of Ag no forward scattering is observed, since for layer-by-layer growth there are no scatterers above the smooth layer of emitters. After deposition of the second layer the emission along the ⟨110⟩ directions appears. At 4.0 ML all the expected forward-scattering directions (compare to Fig. 2) can be identified. The picture sharpens somewhat for the thick 9.1 ML film, proving the good fcc order of the film. The development of the Kikuchi bands can clearly be seen. This ADP is the mirror image of the Pd(111) pattern (compare to Fig. 3), which indicates the twin orientation of the Ag film. From the triangle of the ⟨110⟩ directions it can be clearly seen that the stacking fault is already present at 1.8 ML. A LEED study[13] has proved that the first Ag layer grows pseudomorphically, implying that the stacking fault develops between the first and second layers and not between the Pd substrate and the first layer.

In the bottom row of Fig. 4 ADP's for Au, coverages between 0.8 and 4.5 ML on Ag(111) are shown. For 0.8 ML Au, intensity maxima along the ⟨110⟩ directions can be observed and already a weak enhancement along the ⟨112⟩ directions is visible. Therefore, layer-by-layer growth of Au on Ag(111) can be excluded. Furthermore, the ADP's yield the information that the Au film has fcc lattice structure and grows with the orientation and the stacking of the Ag(111) substrate in accordance with the LEED results.[7]

The ADP's of Au on Ag(111) for coverages of 0.8 ML and 2.0 ML reveal rather high noise. For the presentation of the ADP's we use the whole range of gray shades by showing the lowest intensity as black and the highest intensity as white. A picture with low contrast (difference between highest and lowest intensity normalized to the highest intensity) would, therefore, appear "noisy."

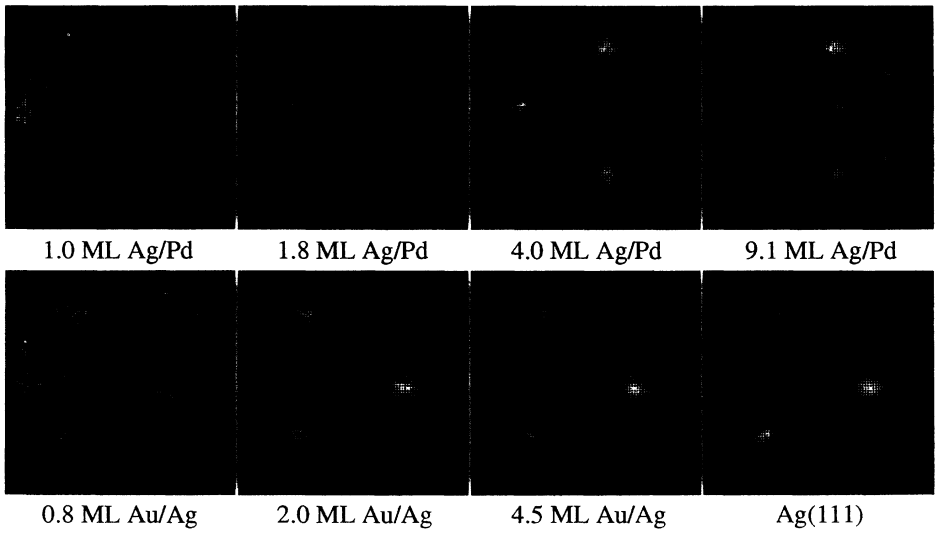

FIG. 4. Experimental angular distributions of photoelectrons for Ag on Pd(111) (top row) and for Au on Ag(111) (bottom row). The coverage increases from left to right. The patterns show the emission from the adsorbate layer except for the clean Ag(111) substrate (lower right corner). The kinetic energies for the Ag $3d$ and Au $4f$ core levels are 519 and 810 eV, respectively.

The original data show that the contrast of the ADP for 0.8 (2.0) ML Au on Ag is similar to the contrast for 1.8 (3.0) ML of Ag on Pd. If Au grew in simultaneous multilayers on Ag(111) with a Poisson distribution of the terrace heights, there would be 35% (69%) of the atoms below other atoms at 0.8 (2.0) ML coverage which would contribute to the contrast. For the layer-by-layer growth observed for Ag on Pd(111), 44% (67%) of the atoms are below other atoms at 1.8 (3.0) ML coverage and contribute to the contrast. The experimental values for the contrast are, therefore, compatible with diffusion-limited simultaneous multilayer growth. The poor statistics of the ADP's for Au on Ag(111) in Fig. 4 must consequently be due the small angle-integrated photoelectron intensity (see Fig. 1). The small Au $4f$ intensity on Ag(111) can be explained only if a considerable number of Au atoms are located in deeper layers. The respective morphology can be explained either by an alloy formation or by the growth of high islands. The latter has already been excluded from the angle-integrated data in Sec. III A and would also yield a much higher contrast than observed and expected for a Poisson distribution of the terrace heights. The "high island model" is also at variance with the result of a high-energy ion scattering study[8] which is particularly sensitive for the detection of high islands. We conclude that an intermixing occurs during the growth of Au on Ag(111) and that Au atoms are incorporated into deeper layers.

C. Au on Ag films on Pd(111)

The conclusions about an intermixing between Au and Ag at room temperature can be confirmed by experiments for deposition of Au on thin Ag films grown on Pd(111). The results for an 8 ML thick Ag film are identical to those for the Ag(111) substrate. This is not surprising, since the surface of such a Ag film is identical to the single-crystal surface (see the right column of Fig. 4 and Refs. 13 and 14). We conclude that there is no significant penetration of Au into Ag(111) beyond 8 ML at room temperature, in agreement with the alloy model of Sec. III C.

The ADP's for $\sim$ 1, 2, and 3 ML of Au deposited on 1.0 and 2.0 (2.7 for 3 ML Au) thick Ag films are shown in Fig. 5. The left column of each half of the figure shows the Au $4f$ intensity distribution which should be compared to the patterns for Au on Ag(111) in the bottom row of Fig. 4. The right column of each half of the figure shows the Ag $3d$ intensity distribution to be compared to the patterns for Ag on Pd(111) in the top row of Fig. 4. If Au continued the layer-by-layer growth of Ag on Pd(111), we would expect a uniform distribution for the 1 ML Au emission, at variance with the observation in Fig. 5 (top row). A close inspection reveals that in all patterns of Fig. 5 emission from atoms two and three layers deep can be seen. The main difference between deposition on 1 ML and 2 ML Ag films is the sixfold symmetry in the former and the threefold symmetry in the latter case. The threefold pattern has the same orientation as for Ag on Pd(111), i.e., with a stacking fault near the interface. The sixfold pattern could be explained by a series of fcc stacking faults (in a hcp-like structure) or by a mixture of two fcc domains. A hcp-like structure would lead to additional forward-scattering directions[19] which are not observed. The occurrence of only the fcc structure in two domains seems more likely, since Ag-Au alloys exhibit a fcc structure independent of concentration.[33] A precoverage by a smooth monolayer of Ag is obviously penetrated by the Au, leading to two fcc domains, which could be explained by several-layer-high Ag islands (showing a stacking fault) and Au islands (with the regular fcc stacking). Since both the Ag and the Au emission show the sixfold pattern both types of islands must contain Ag and Au, and differ mainly in the layer connected to the Pd(111) substrate. Note that Au grows on Pd(111) in the fcc structure without a stacking fault.[25] We would like to point out that a precoverage of 2 ML of Ag is sufficient to preserve the stacking fault which develops between the first two Ag layers and accommodates the strain due to the lattice mismatch.[13,34]

The data indicate that the mixed zone is not extended

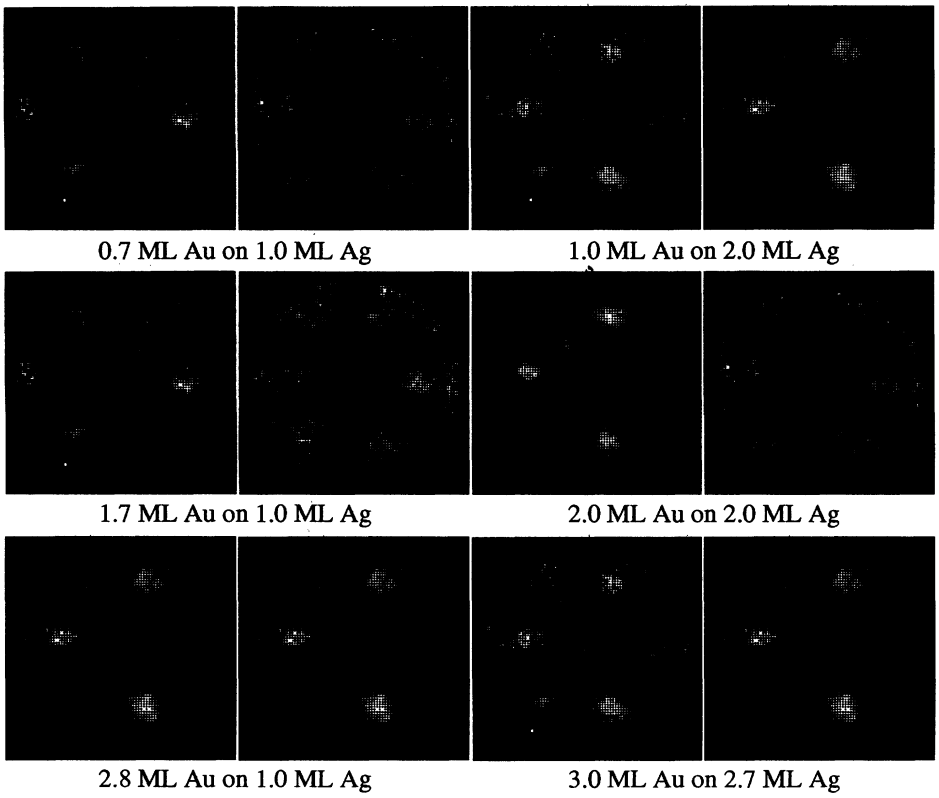

FIG. 5. Experimental angular distributions of photoelectrons for Au films of various thicknesses deposited at room temperature on 1.0 ML (left half) and 2.0 or 2.7 ML (right half) of Ag on Pd(111). In each half of the figure the left column shows the Au $4f$ intensity at 810 eV kinetic energy and the right column the Ag $3d$ intensity at 519 eV kinetic energy.

over more than one or two layers, since with increasing Au coverage the angle-integrated photoelectron intensity of Ag decreases and of Au increases. The alloy model of Sec. III C predicts a strongly intermixed zone extended over ≈ 3 layers. This is no contradiction, since the boundary conditions for diffusion into a Ag layer of finite thickness are different. The diffusion of Au into the compressed pseudomorphic first Ag layer on Pd(111) might also be different from the diffusion into Ag(111). The onset of intermixing around 275 K has been observed for monolayers of Ag and Au deposited on Ru(0001) by Wandelt *et al.*[35]

V. DISCUSSION

The growth behavior of a metal-on-metal system is determined by energetic and kinetic factors. The system tends to form the energetically most favorable configuration. This often cannot be reached due to kinetic limitations, since the growth conditions are usually far from thermodynamic equilibrium. The energetic requirement for layer-by-layer growth to occur is that the sum of the film surface free energy plus the interfacial energy must be smaller than the substrate surface free energy.[1] The calculated surface free energy values for Au(111), Pd(111), and Ag(111) are 0.79, 1.22, and 0.62 J/m^2, respectively.[36] These values correctly predict the layer-by-layer growth for Ag on Pd(111). For Au(111) and Ag(111) the surface free energies are almost equal. A prediction of the growth mode depends, therefore, critically on the value for the interfacial energy. Due to the small lattice mismatch between Au and Ag the films are practically stress-free and the associated term in the interfacial energy can be neglected. Silver and gold are miscible at all concentrations and the reaction of the Ag-Au alloy formation is exothermic. Consequently, the interfacial energy is negative. Values found in the literature are -0.39 J/m^2,[37] -0.23 J/m^2,[36] and -0.10 J/m^2.[38] The sum of the surface free energy for Au(111) and the interfacial energy is almost equal to the surface free energy for Ag(111), independent of the choice for the value of the interfacial energy.

Even though a reliable prediction for the growth mode seems impossible, the exothermic Au-Ag reaction indicates that the formation of an alloy at the interface with its increased number of Au-Ag bonds might be energetically favorable. This is in agreement with the intermixing observed for Au on the open Ag(110) surface.[4] It has been reported that, during the growth of Au on Ni(110), Au atoms are incorporated into the Ni(110) surface at low coverages.[6] Gold and nickel are immiscible and have a large lattice mismatch. The effect was explained by the lowering of the energy due to the formation of Au-Ni bonds compared to undercoordinated Au atoms sitting on the surface. The tendency of the Au surfaces to form reconstructions with an increased density of atoms in the top layer[39,40] indicates also that undercoordinated Au atoms are energetically unfavorable. It seems, therefore, plausible that Au atoms arriving on the Ag(111) surface are incorporated into the surface, thereby gaining energy in three different ways: (i) by reducing the number of unsaturated bonds compared to Au atoms staying on the surface, (ii) by maximizing the number of Au-Ag bonds,

and (iii) by lowering the surface free energy by increasing the Ag coverage in the top layer. These energy considerations would favor a Ag-rich surface, which would be compatible with the results of Lipphardt *et al.*[12] who observe almost no changes in some of their data for coverages up to 5 ML. Our TDS data and the ion scattering data of Mahavadi,[10] however, do not indicate a Ag-rich surface layer.

The question remains, how does this alloy formation take place on a close-packed surface? Our forward-scattering results show conclusively that Au atoms are incorporated at least down to the third layer. At room temperature bulk diffusion has been excluded.[41] This leaves diffusion or exchange processes at the surface as the only possible mechanisms. With pure lateral diffusion Au atoms can be buried only in the presence of steps at the surface. Such a mechanism has been proposed by Rousset *et al.*[4] for Au on Ag(110). The direct exchange of a Au atom with a Ag atom on a (111) terrace seems unlikely at first sight. However, the energy for a vacancy formation at a Ag(111) surface is relatively low compared to other surfaces.[42] This energy could be regained by filling the vacancy with the Au atom. This process might work even more efficiently near a step edge where the ejected Ag atom can be rebound. In order to bury Au atoms several layers deep, a combination of exchange and diffusion must be operative. The importance of the effect of steps and defects on the growth behavior has been pointed out by Meinel, Klaua, and Bethge.[9] This and the onset of diffusion of Au into the bulk just above room temperature[31] might also be the explanation for the contradictory results in the literature.

VI. CONCLUSIONS

In summary, we have performed a forward-scattering experiment, combined with XPS analysis and TDS of NO, of thin Au films deposited onto Ag(111) surfaces at room temperature. All of the three investigation methods lead to a conclusive result about incorporation of Au in the Ag(111) surface. It would be worthwhile to study the growth of Au on Ag(111) with scanning tunneling microscopy to clarify the mechanism of the Au incorporation and the influence of steps in more detail.

ACKNOWLEDGMENTS

We acknowledge stimulating discussions with Professor W. Steinmann and Professor A. Goldmann. We are grateful to Professor E. Bauer for making the thesis of P. Mahavadi available to us. This work was supported by the German Federal Minister of Research and Technology (Grant No. BMFT 05 464 AAB 2).

[1] E. Bauer, Z. Kristallogr. **110**, 372 (1958); Appl. Surf. Sci. **11/12**, 479 (1982).
[2] D. D. Chambliss, K. E. Johnson, R. J. Wilson, and S. Chiang, J. Magn. Magn. Mater. **121**, 1 (1993).
[3] C. Günther *et al.*, Ber. Bunsenges. Phys. Chem. **97**, 522 (1993).
[4] S. Rousset, S. Chiang, D. E. Fowler, and D. D. Chambliss, Phys. Rev. Lett. **69**, 3200 (1992).
[5] H. Röder, R. Schuster, H. Brune, and K. Kern, Phys. Rev. Lett. **71**, 2086 (1993).
[6] L. Pleth Nielsen *et al.*, Phys. Rev. Lett. **71**, 754 (1993).
[7] F. Soria, J. L. Sacedon, P. M. Echenique, and D. Titterington, Surf. Sci. **68**, 448 (1977).
[8] R. J. Culbertson, L. C. Feldman, P. J. Silverman, and H. Boehm, Phys. Rev. Lett. **47**, 657 (1981).
[9] K. Meinel, M. Klaua, and H. Bethge, J. Cryst. Growth **89**, 447 (1988).
[10] P. Mahavadi, Ph.D. thesis, University of Clausthal, 1989.
[11] B. Gruzza, J. M. Guglielmacci, and M. Gillet, Thin Solid Films **52**, 167 (1978).
[12] U. Lipphardt *et al.*, Surf. Sci. **294**, 84 (1993).
[13] B. Eisenhut, J. Stober, G. Rangelov, and Th. Fauster, Phys. Rev. B **47**, 12 980 (1993).
[14] R. Fischer *et al.*, Phys. Rev. Lett. **70**, 654 (1993).
[15] W. F. Egelhoff, Jr., Crit. Rev. Solid State Mater. Sci. **16**, 213 (1990).
[16] C. S. Fadley, in *Synchrotron Radiation Research: Advances in Surface Science*, edited by R. Z. Bachrach (Plenum, New York, 1992), Chap. 11.
[17] S. A. Chambers, Adv. Phys. **40**, 357 (1991).
[18] J. Osterwalder, Arab. J. Sci. Eng. **15**, 273 (1990).
[19] Th. Fauster, G. Rangelov, J. Stober, and B. Eisenhut, Phys. Rev. B **48**, 11 361 (1993).
[20] J. Osterwalder, T. Greber, A. Stuck, and L. Schlapbach, Phys. Rev. B **44**, 13 764 (1991).
[21] D. Rieger, R. D. Schnell, W. Steinmann, and V. Saile, Nucl. Instrum. Methods Phys. Res. **208**, 777 (1983).
[22] R. G. Musket *et al.*, Appl. Surf. Sci. **10**, 143 (1982).
[23] M. P. Seah and W. A. Dench, Surf. Interface Anal. **1**, 2 (1979).
[24] S. Ossicini, R. Memeo, and F. Ciccacci, J. Vac. Sci. Technol. A **3**, 387 (1985).
[25] B. Eisenhut, Ph.D. thesis, University of Munich, 1993.
[26] M. E. Bartram and B. E. Koel, Surf. Sci. **213**, 137 (1989).
[27] P. J. Goddard, J. West, and R. M. Lambert, Surf. Sci. **71**, 447 (1978).
[28] D. A. Outka and R. J. Madix, Surf. Sci. **179**, 351 (1987).
[29] W. Hansen, M. Bertolo, and K. Jacobi, Surf. Sci. **253**, 1 (1991).
[30] J. Crank, *The Mathematics of Diffusion* (Oxford University Press, London, 1985).
[31] K. Meinel, M. Klaua, and H. Bethge, Ultramicroscopy **20**, 261 (1986).
[32] D. Naumović *et al.*, Phys. Rev. B **47**, 7462 (1993).
[33] P. Wiest, Z. Phys. **81**, 121 (1933).
[34] H. Brune, H. Röder, C. Boragno, and K. Kern (unpublished).
[35] K. Wandelt, J. W. Niemantsverdriet, P. Dolle, and K. Markert, Surf. Sci. **213**, 612 (1989).
[36] S. M. Foiles, M. I. Baskes, and M. S. Daw, Phys. Rev. B

33, 7983 (1986).
[37] A. R. Miedema, P. F. de Châtel, and F. R. Boer, Physica B&C **100B**, 1 (1980).
[38] R. Hultgren *et al.*, *Selected Values of the Thermodynamic Properties of Binary Alloys* (American Society for Metals, Metals Park, OH, 1963).
[39] U. Harten, A. M. Lahee, J. P. Toennies, and C. Wöll, Phys. Rev. Lett. **54**, 2619 (1985).
[40] M. A. van Hove *et al.*, Surf. Sci. **103**, 189 (1981).
[41] M. H. Yang and C. P. Flynn, Phys. Rev. Lett. **62**, 2476 (1989).
[42] H. M. Polatoglou, M. Methfessel, and M. Scheffler, Phys. Rev. B **48**, 1877 (1993).

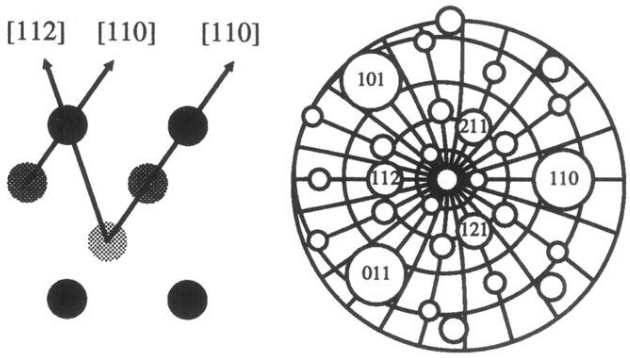

FIG. 2. (Left) Side view normal to the (111) surface of a fcc crystal [$(1\bar{1}0)$ plane] to illustrate the dense packed, low-index crystallographic directions which correspond to the expected intensity maxima in the forward-scattering experiment. (Right) The expected angular distribution of photoelectrons for a fcc (111) surface due to the forward scattering of the electrons by the neighbor atoms along the crystal directions given by the numbers. The center of the angular grid corresponds to normal emission [(111) direction]. The separation between the lines of the grid is 10° and 15° for the polar and azimuthal directions, respectively.

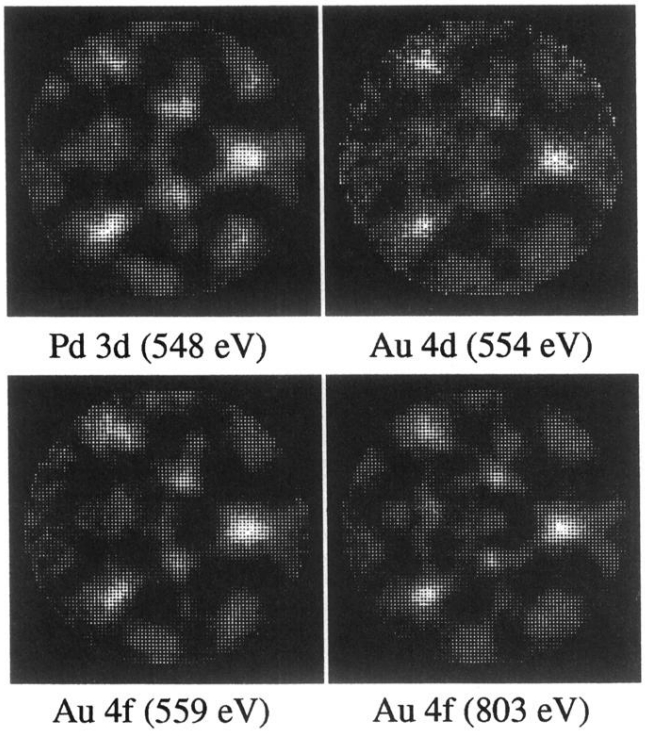

FIG. 3. Comparison of the experimental angular distributions of photoelectrons for different core levels Pd 3*d*, Au 4*d*, and Au 4*f* at a kinetic energy around 550 eV. For a kinetic energy of 803 eV the forward scattering becomes more pronounced. The data were obtained for the clean Pd(111) surface and for an 8 ML thick Au film on Pd(111).

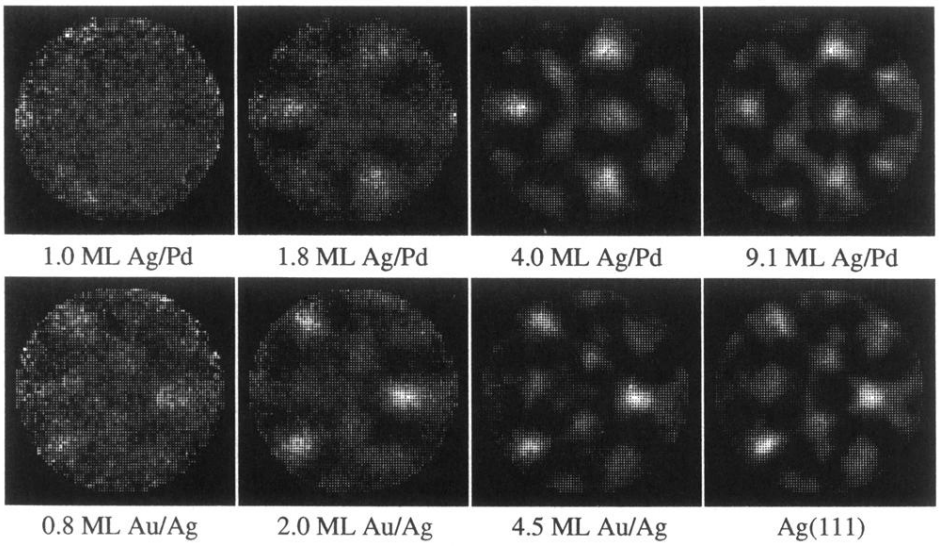

FIG. 4. Experimental angular distributions of photoelectrons for Ag on Pd(111) (top row) and for Au on Ag(111) (bottom row). The coverage increases from left to right. The patterns show the emission from the adsorbate layer except for the clean Ag(111) substrate (lower right corner). The kinetic energies for the Ag $3d$ and Au $4f$ core levels are 519 and 810 eV, respectively.

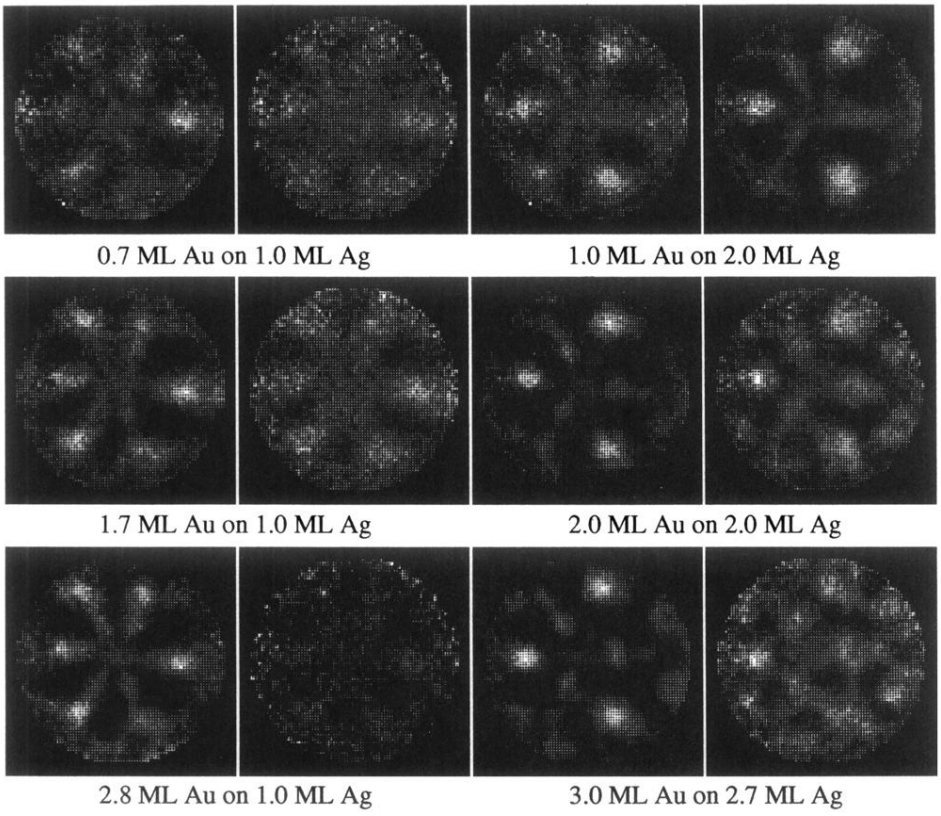

FIG. 5. Experimental angular distributions of photoelectrons for Au films of various thicknesses deposited at room temperature on 1.0 ML (left half) and 2.0 or 2.7 ML (right half) of Ag on Pd(111). In each half of the figure the left column shows the Au $4f$ intensity at 810 eV kinetic energy and the right column the Ag $3d$ intensity at 519 eV kinetic energy.